

Shear strengthening of reinforced concrete beams using externally-bonded aluminum alloy plates: An Experimental Study

Jamal A. Abdalla^{1*}, Adi S. Abu-Obeidah², Rami A. Hawileh³, Hayder A. Rasheed⁴

Abstract

Recently developed high strength Aluminum Alloys (AA) have desirable characteristics that make them attractive as externally bonded strengthening materials. This paper investigates the potential of using AA plates for shear strengthening of reinforced concrete (RC) beams. Five shear deficient RC beams were externally strengthened using AA plates with different orientations. It is observed that the shear capacity of the strengthened beams has increased in the range of 24%-89% compared to the un-strengthened beam. Shear capacity of the strengthened beams was also predicted using the ACI440, FIB14, TR55 and SMCFT design guidelines with the later one giving the most accurate predictions.

Keywords: Aluminum alloy; externally-bonded material; shear deficient beams; FRP.

1. Introduction

There is a considerable number of RC structures around the world, that can no longer be considered safe [1], as they deteriorated over the years due to various environmental factors, including carbonation, chloride attack, corrosion, etc. As a result, these structures either need to be replaced, which is costly, or strengthened using new and innovative materials. Also, the increase in live loads due to change in building functionality and traffic load demand on bridges, made it necessary to consider strengthening and retrofitting of such structures. The strengthening

¹ Professor, Department of Civil Engineering, American University of Sharjah, UAE.

* corresponding author email: jabdalla@aus.edu

² Graduate Student, Department of Civil Engineering, Rutgers, The State University of New Jersey, NJ, USA.

³ Professor, Department of Civil Engineering, American University of Sharjah, UAE.

⁴ Professor, Department of Civil Engineering, Kansas State University, Manhattan, KS, USA.

methods implemented should be simple, effective and economical to be considered as viable option. Strengthening of shear deficient reinforced concrete beams today are mainly accomplished by externally bonding steel plates or transverse fiber reinforced polymer (FRP) sheets or plates to the web faces of these beams. The choice of FRP sheets and plates in shear strengthening of structural concrete members were investigated by many researchers and proved to be effective [2-20]. Also, the use of steel plates as externally bonded material has proven to be effective as investigated by other researchers [1, 21-25].

Alternatively, Aluminum Alloy (AA) has the desirable mechanical properties that can overcome some deficiencies in steel and FRP and qualifies it as a superior external strengthening material. As a result, this study is mainly focused on experimentally investigating the potential of using aluminum alloys as externally bonded strengthening material. The recently developed aluminum alloys possess desirable characteristics that can overcome the deficiencies in steel and FRP. These alloys are economical, effective and easy to install as demonstrated by a preliminary study conducted by the authors [26-28] to proof the concept. To the best of the authors' knowledge, the use of AA plates as externally bonded strengthening material has not been investigated, yet. Therefore, the significance of this research is to investigate the feasibility and the effectiveness of using AA plates in external shear strengthening of deficient reinforced concrete beams

2. Background

A brief background of the experimental investigations in shear strengthening of RC beams using FRP and steel is given below, along with an introduction of the superior advantages of using AA plates.

2.1 Shear Strengthening using FRP

In the last two decades, extensive research on shear strengthening of RC beams using externally bonded CFRP and GFRP composite materials have been conducted by many researchers [2, 6, 11-13, 15, 29-31]. The shear strengthening methods employed, involve side bonding of sheets or plates and U-wrapping of sheets at different orientations and configurations. The results showed that there is a considerable increase in the shear capacity of deficient beams exceeding 90% [29]. Hawileh et al. [32, 33] and Nawaz et al. [34] investigated the effect of longitudinal flexural reinforcement of CFRP sheets and plates on shear capacity of RC beams. They concluded that the increase in the capacity of the specimens strengthened with longitudinal CFRP sheets was in the range of 10% to 70% [32] and for those strengthened with longitudinal CFRP plates was in the range of 13% to 138% [34] compared to the control specimens. The effect of U-jacketing or U-wrapping using CFRP and GFRP sheets on shear strengthening of RC beams was also studied by several investigators [2, 6, 11, 12, 16, 35-37]. They concluded that FRP sheet U-Wrapping significantly increases the shear capacity of deficient beams. The U-wrap with end anchorage was shown to be the most effective configuration in increasing shear capacity [6]. Shear strengthening of RC beams subjected to cyclic loading was conducted by Calalillo and Sheikh [14] who concluded that using CFRP sheets was effective in increasing the capacity of the under designed beams in the range of 25% to 114%.

2.2 Shear Strengthening using steel plates

Other researchers have also studied the use of steel plates in shear strengthening of RC beams [1, 22-25, 38]. Adhikary et al. [1] and Adhikary and Mutsuyoshi [23] studied the effect of epoxy-bonded continuous horizontal steel plates with different thickness and width on the shear capacity of beams under-reinforced in shear. They observed that continuous steel plates bonded

externally to beam webs showed shear strength levels 84% higher than the respective values of the control beam. In another study, Adhikary and Mutsuyoshi [24] examined the effect of different strengthening schemes and techniques including steel strips, externally anchored steel stirrups, small plates of steel and steel brackets on the under-reinforced shear capacity improvements. They observed that epoxy bonded steel plates provided around 72% increase in shear capacity, while beams with externally anchored stirrups yielded 117% increase in shear capacity compared to the control beam. Barnes et al. [22] tested several beams to investigate the effect of externally bonded and anchored steel plates in the shear capacity improvement of RC beams. They investigated different (a) plate thicknesses, (b) shear span-to-depth ratios and (c) connections to the beam's side surfaces. The ultimate capacity of the beams with bonded plate was increased up to 90% compared to the control beam. Altin et al. [38] investigated the effect of side bonded steel plates on the shear capacity of RC T-beams. All the plates were bonded using epoxy adhesive along the shear span of the beam web. The results showed that the externally bonded steel plates improved beams strength, stiffness and ductility. The increase in the shear capacity of the RC beams ranged between 88% and 98% of the control beam. Barnes and Mays [25] tested several R/C rectangular beams and T- beams strengthened with steel plates and steel links bonded with epoxy adhesive. The increase in the shear capacity of the rectangular beams ranged between 30% and 194% and for the T-beams from 5% up to 88%.

2.3 Aluminum Alloys

Although FRP and steel materials have proven to be very effective in shear strengthening of RC beams, however, they have their unavoidable shortcomings. For instance, the disadvantages of using steel plates as externally bonded material are their low corrosion resistance, heavy weight and the need for coating and painting that result in high maintenance

cost [39]. Also, the weaknesses of FRP materials are their low thermal resistance, brittle behavior with no well-defined yield point and the unidirectional properties that limit their use. Recently developed high strength aluminum alloys are some of the most promising metals that can be bonded externally to structural elements and contribute significantly in increasing their load carrying capacity while overcoming some of the drawbacks of using FRP and steel. Some of the desirable characteristics and compelling reasons for using aluminum alloys in particular as externally bonded strengthening material are their high strength to weight ratio, high ductility, high corrosion resistance, high thermal resistance and their reasonable cost. Aluminum is an isotropic material that is easy to form and easy to bond to RC surface using epoxy with or without mechanical anchorages.

Until recently, aluminum alloys are used predominantly in the aerospace industry and in ship-buildings. In recent years, aluminum alloys found applications in pedestrian bridges and in some light structures. The recent development of high strength aluminum alloys [40, 45] and the reduction in cost have encouraged structural engineers to consider aluminum alloy in several other applications.

There are different types of aluminum alloy materials that belong to eight different series (1000 -8000 series). The 5000 series (e.g., 5083 and 5086) are called marine grade aluminum alloy. These are mainly used in ship-buildings and pressure vessels and they are available in sheet forms. Their ultimate tensile strength ranges between 275 - 350 MPa. The 6000 series, e.g., 6061, 6063 and 6082 are called structural aluminum alloy and are used for structural components. Their ultimate strength reaches 300 MPa. The 7000 series, e.g., 7068, 7075 are of high strength and are used in aircraft and aerospace industries. Their ultimate tensile strength reaches 570 MPa. In addition, the newly developed 2000 series (e.g., 2524, 2224), 7000 series

(e.g., 7475, 7055) and new generation aluminum–lithium (Al–Li) alloys (e.g., 2050, 2099) [40-45] with high tensile strength, among other desirable characteristics, are very promising as externally bonded strengthening materials [46].

The material used in this investigation is annealed wrought AA5083-0, available in sheets and plates, and has been selected for its exceptional performance in extreme environments [45], such as seawater and industrial chemicals. Furthermore, it has the highest strength among the non-heat treatable alloys. The chemical composition, physical and mechanical properties of AA5083-0 are shown in Table 1. This type of aluminum alloy is typically used in shipbuilding, rail cars, vehicle and truck bodies, dump truck boxes, storage tanks and pressure vessels [45]. AA5083-0 ultimate tensile strength ranges between 290-294 MPa, its tensile yield strength ranges between 145-147 MPa, its modulus of elasticity is 70 GPa and its elongation at break is around 22%.

Table 1 Chemical composition, physical and mechanical properties of 5083-0 AA [45]

Chemical Composition		Physical and Mechanical Properties	
Chemical element	% Present	Property	Value
Aluminum, Al	92.4 – 95.6%	Density	2.65 g/cm ³
Chromium, Cr	0.05-0.25	Melting Point	570 °C
Copper, Cu	≤ 0.1%	Thermal Expansion	25 x10 ⁻⁶ /K
Iron, Fe	≤ 0.4%	Modulus of Elasticity	72 GPa
Magnesium, Mg	4 – 4.9%	Thermal Conductivity	121 W/m.K
Manganese, Mn	0.4 – 1 %	Electrical Resistivity	0.058 x10 ⁻⁶ Ω .m
Others, each	≤ 0.05%	Proof Stress	145 MPa
Others, total	≤ 0.15%	Tensile Strength	300 MPa
Silicon, Si	≤ 0.40%	Elongation A50 mm	23 %
Titanium, Ti	≤ 0.15%	Shear Strength	175 MPa
Zinc, Zn	≤ 0.25%	Hardness Vickers	75 HV

3. Experimental Program

3.1. Materials and Material tests

3.1.1. Concrete

Ready-mixed concrete was used to cast all specimens. Concrete cubes of 150 mm x 150 mm x 150 mm were made from the same batch on site and tested to determine the compressive strength of the concrete. The cubes were tested after 28 days and the average compressive strength of the concrete cubes was found to be equal to 37.2 MPa (equivalent to cylinder strength of around 29.76 MPa).

3.1.2. Steel Bar Reinforcement

To determine the mechanical properties of reinforcing steel used in this study, three steel reinforcing bars were tested under uniaxial tension. The total length of the specimens was 300 mm with a gauge length of 100 mm. The obtained results for the elastic modulus (E_s), yield strength (f_y), and tensile strength (f_u) are presented in Table 2. Fig. 1 shows the stress-strain curves of the tested specimens.

Table 2 Steel reinforcements bars properties

	E_s (GPa)	f_y (MPa)	f_u (MPa)
Specimen#1	199.99	588.5	694.0
Specimen#2	199.97	587.4	698.8
Specimen#3	200.00	595.05	711.3
Average	199.99	590.36	701.40

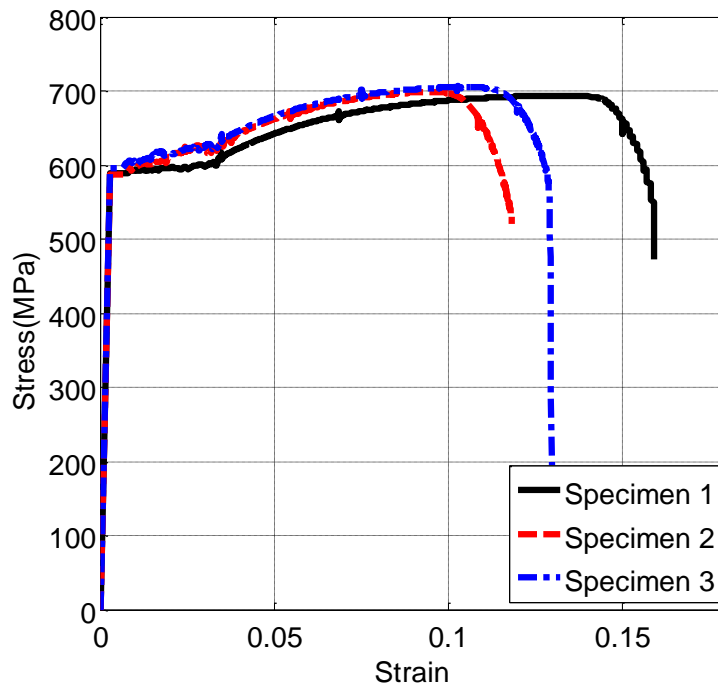


Fig. 1. Test results of steel reinforcement

3.1.3. AA5083-0 Plates

To determine the mechanical properties of AA5083-0 used in this study, three specimens were shaped as a dogbone coupon and tested using ASTM B928/B928M [47] standard specifications for high Magnesium Aluminum-Alloy sheet and plate for Marine service and similar environments. As shown in Fig. 2, the plates were machined to enforce failure in the specimen away from the grips. The specimens were prepared according to the ASTM standards [47]. Each coupon specimen had a total length of 300 mm, width of 45 mm, radius of fillet of 12.5 mm, grip length of 50 mm, and a gauge length of 100 mm as shown in Fig. 2a. Fig. 2b shows the test setup in a 100 kN Universal Testing Machine (UTM) that has gripped the specimen from both sides. Fig. 2c and Fig. 2d show the three prepared specimens that are labeled as A1, A2 and A3 before and after testing, respectively. The failure plane of the three specimens occurred within the gauge length (i.e., machined part).

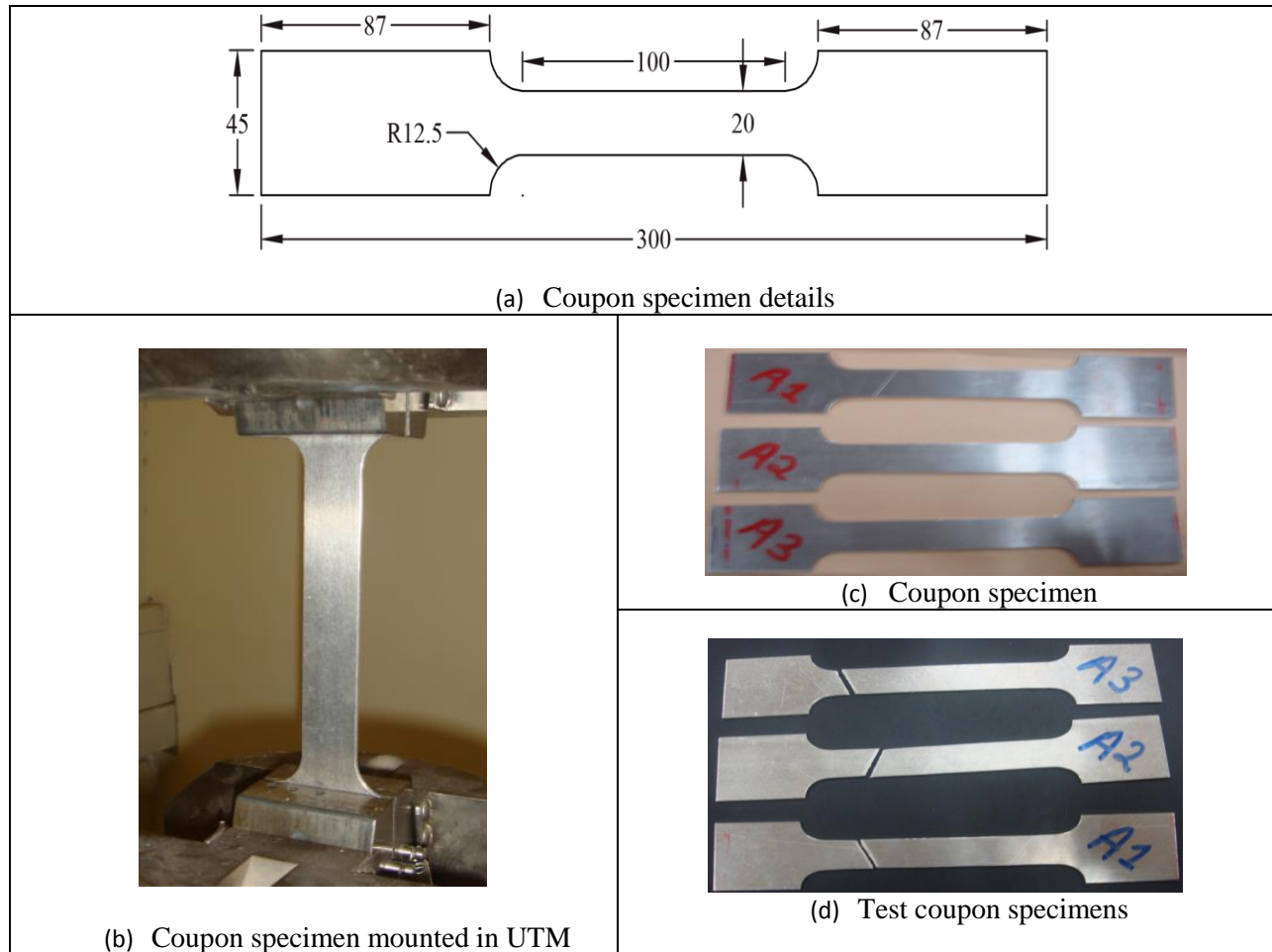


Fig. 2. Coupon test of aluminum alloy specimens

Fig. 3 and Table 3 present the tensile test results for the three AA5083-0 specimens. The measured average yield strength was 146.3 MPa, the measured average ultimate strength was 293 MPa and the measured average elongation at break was 24.3% which are in close agreement with those of the manufacturer's specifications [45].

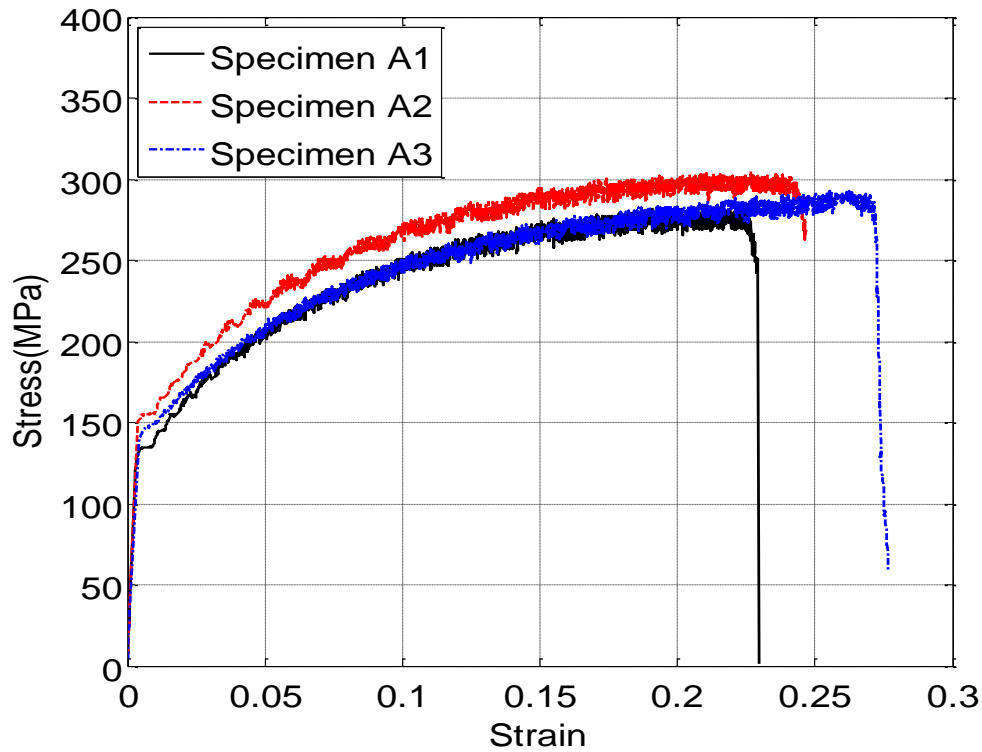


Fig. 3. Stress-strain curve of the tested AA5083-0 specimens

Table 3 Mechanical properties of the tested AA5083-0 specimens

	E_{AA} (GPa)	f_y (MPa)	f_u (MPa)	Elongation (%)
Specimen A1	-	141	281.87	22.34
Specimen A2	-	150	304.42	23.94
Specimen A3	-	148	292.78	26.71
Average of tests	-	146.3	293.0	24.3
Specifications	70	145	295	22

3.1.5. Epoxy

Sikadur-30LP [48] is the epoxy resin adhesive used in this study to bond the AA plates to the concrete surfaces. It is solvent-free, structural two-part adhesive (part A and part B) that has been designed for use at temperatures between 25° C and 45° C for bonding structural strengthening reinforcements. It is easy to mix and easy to apply, doesn't require primer installation and is suitable for dry and damp concrete surfaces. To create the adhesive mix, part

A and part B needed to be mixed in a ratio of 3:1 continuously for a 3-4 minute period until a light grey color emerged. After getting the light grey color, the epoxy must be used within 45 minutes which is the time needed to dry. After a curing time of 7-14 days in a room temperature of 25°C, the modulus of elasticity, compressive strength, flexure strength and shear strength of the cured epoxy were 10 GPa, 85 MPa, 25 MPa, and 17 MPa, respectively. The epoxy had a density of 1.8kg/ltr +/- 0.01 kg/ltr and its measured thickness is usually between 1-3 mm. Its hardening is not affected by high relative humidity, and it is impermeable to liquids and water vapor. To ensure the maximum bond strength, concrete surface and aluminum plates were all grinded to achieve adequate bond strength between them. Table 4 summarizes some of the physical and mechanical properties of the epoxy as reported by the manufacturer [48].

Table 4 Technical data of Sikadur-30 LP CFRP laminate (plate) epoxy [48]

Property	Description (value or range)
Appearance and colors	Resin part A: white, Resin part B: black Part A+B mixed: light grey
Service temperature	- 40°C to + 45°C (when cured at > +23°C)
Density	1.65 kg/ltr + 0.1 kg/ltr (parts A+B mixed at +23°C)
Tensile strength	15 to 18 MPa (7 days curing time at +25°C)
Flexural strength	> 25 MPa (7 days curing time at +25°C)
Compressive strength	> 85 MPa (3 days curing time at +25°C)
Bond strength	Concrete fracture (> 4 MPa) on sand-blasted substrate: > 1 day
Shear strength	7 MPa (7 days curing time at +25°C)
Change of volume	Shrinkage: 0.04%
Thermal stability	Heat Distortion Temperature (HDT): + 47°C (7 days at +23°C)
E-modulus	Compression: 10 GPa (7 days at +25°C) Tensile: 10GPa (7 days at +25°C)
Mixing	Part A : Part B = 3 : 1 by weight or volume

Table 5 provides a summary of the average values of the important mechanical material

properties of concrete, steel reinforcement, AA, and epoxy used and explained earlier in the experimental program of this study.

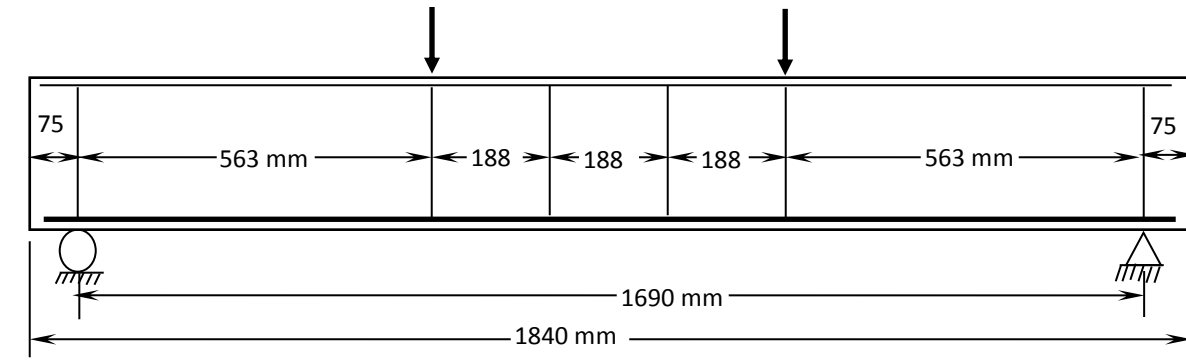
Table 5 Summary of mechanical material properties

Concrete		Steel		AA5083-0					Epoxy	
f_{cu} (MPa)	E_c (GPa)	f_y (MPa)	E_c (GPa)	E_{AA} (GPa)	ϵ_{AA} (%)	f_y (MPa)	f_t (MPa)	Thicknes s (mm)	E_E (GPa)	f_t (MPa)
37.2	28.7	590.4	200	70	24.3	147	293	2.0	10	30

3.2. Specimens details and testing procedure

3.2.1. Specimens' details

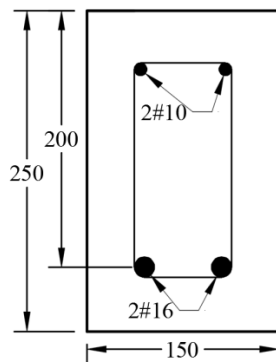
In this study, six shear-deficient reinforced concrete beams were designed, fabricated and tested. Five of these beams were strengthened by externally bonding 2 mm-thick AA plates to the web sides. The dimensions and reinforcement details of the control beam (un-strengthened specimen) are shown in Fig. 4. Each beam specimen has a total depth of 250 mm, width of 150 mm, total length of 1840 mm and a clear span length of 1690 mm. Four point bending was the loading protocol that was monotonically used to failure. The shear span region was extended for 563mm from each support. The beams were cast with no stirrups in the shear span to ensure shear failure of the tested specimens. Four Ø8 mm stirrups were provided only in the constant moment region to easily manufacture the steel cage and also to avoid any stress concentration in the concrete under the loading points (Fig. 4b). All beams were reinforced in flexure with 2Ø16 mm bars with a concrete cover of 42 mm. In the compression zone, the beams were reinforced with 2Ø10 mm bars. Five beams were strengthened in shear using 2 mm thick AA plates (AA5083-0) that were installed on both web sides. The AA plates were bonded on the sides of both shear span regions with different orientations to act as the only shear reinforcement for the beams. Arrangement of the AA plates and the configuration of the strengthening schemes are shown in Fig. 5.



(a)



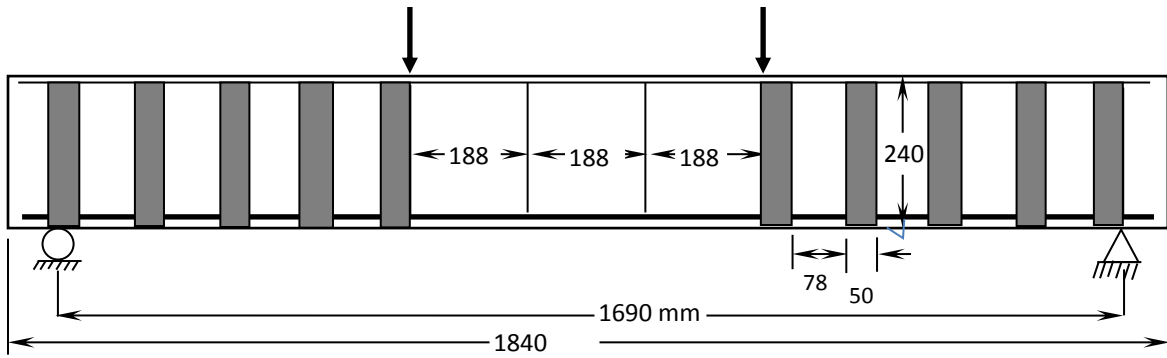
(b)



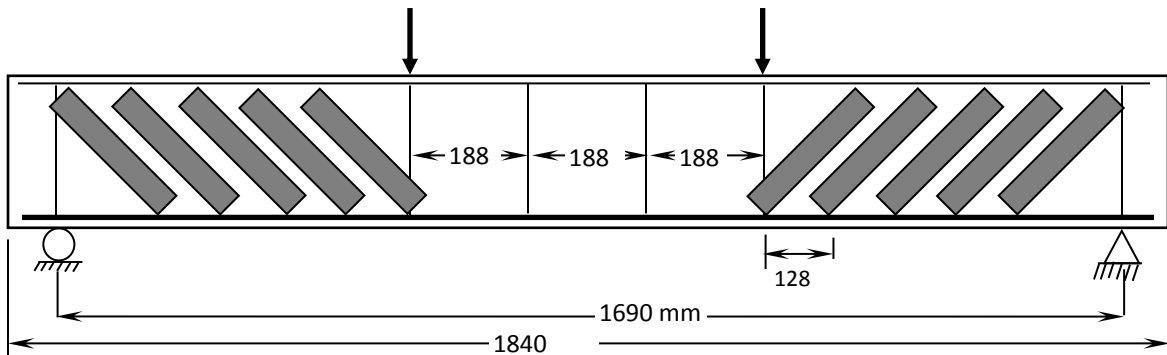
(c)

Fig. 4. Control beam reinforcement profile and cross section

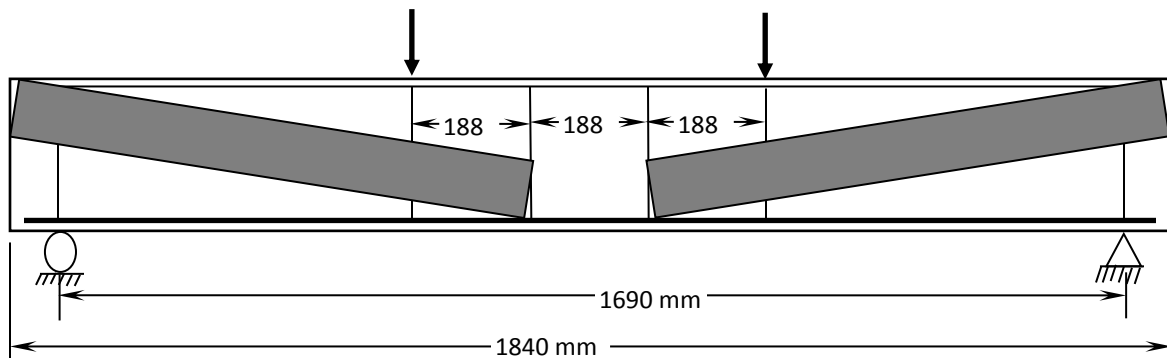
The strengthening procedure of the tested beams included surface preparation by grinding the shear faces of the concrete beam and the back faces of the AA plates with a rotary diamond grinder to create a rough surface and to ensure sufficient bond between them. Once the surface was prepared to the required roughness level, the epoxy resins were applied on both surfaces and the AA plates were pressed in place. Similar strengthening procedure was carried out for all strengthened specimens.



(a)



(b)



(c)

Fig. 5. Details of the strengthened specimens (AA90, AA45, AADP)

Figs. 5a – 5c show the three different orientations for the strengthened specimens which are designated as AA90-1, AA90-2, AA45-1, AA45-2 and AADP. AA90 specimens represent beams that were strengthened with 5 mm x 240 mm vertical (90°) AA strips spaced at 128 mm center-

to-center as shown in Fig. 5a. AA45 specimens represent beams strengthened with the same AA strips used for AA90 beams, bonded at an orientation of 45° and spaced at 128 mm center-to-center as shown in Fig. 5b. Two beams were tested from each of the AA90 and AA45 category. The fifth beam was strengthened with a 10 mm x 790 mm AA plate diagonally bonded (AADP) at an angle of $\pm 10^\circ$ opposite to the shear crack directions as depicted in Fig. 5c.

3.2.2. Testing procedure

The un-strengthened control beam and the five strengthened beams with externally bonded AA plates were all tested under four-point bending monotonically to failure as shown in Figs. 4-5. The control beam was used as a benchmark for comparison with the strengthened beam specimens. The beams were loaded monotonically using, a digitally controlled INSTRON 8806 Universal Testing Machine (UTM), at a rate of 10 kN/min. The loading rate was relatively slow to simulate static loading condition. Foil Strain gauges on some of the aluminum plates were installed to capture the strain response during loading. One strain gauge was installed on the middle plate for the AA90 and AA45 beams from each shear span region and one LVDT was installed at mid-span for all beams to measure deflection. The load was recorded by the UTM machine load cell at 0.1-second time interval and the corresponding mid-span deflection of the beams was recorded at the same rate using the data acquisition system.

4. Results and Discussions

The ultimate load (P_u) and the corresponding ultimate deflection (δ_u) for all the tested beams have been determined. The test results of all specimens will be discussed in this section with respect to their strength, load-deflection response curves, and failure modes. The obtained experimental results for all the tested specimens are summarized in Table 6.

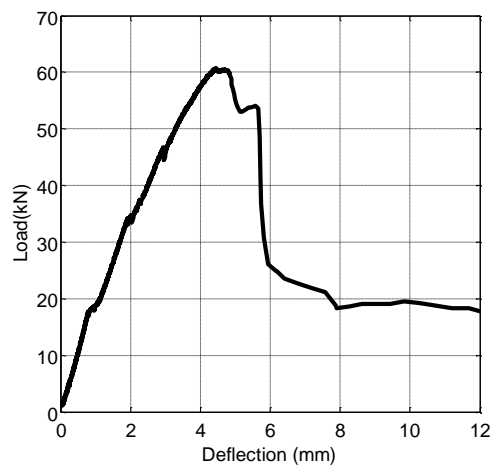
Table 6 Summary of test results and performance comparisons

	P_u	P_u/P_{uCB}	δ_u	Failure mode
CB	60.73	1.00	4.42	Shear
AA90 – 1	106.83	1.76	7.18	Shear
AA90 – 2	75.03	1.24	6.10	Shear
AA45 – 1	114.74	1.89	9.80	Shear/ crushing
AA45 – 2	96.75	1.59	9.60	Shear
AADP	109.55	1.80	7.53	Flexure/ shear

4.1 Control Beam (CB)

4.1.1 Strength and load deflection response

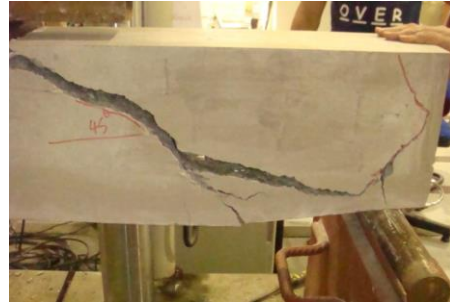
The load versus mid-span deflection response curve for the CB is presented in Fig. 6(a). The ultimate load capacity achieved by the CB beam was 60.73 kN and the corresponding ultimate deflection δ_u was 4.42 mm. Based on the flexural capacity equation of ACI 318-14 code, the calculated ultimate load capacity of the control beam is 59.16 kN which is 97% of the measured experimental value.



(a) Load-deflection



(b) cast specimen



(c) Failure mode

Fig. 6. Control Beam (CB) details and results

4.1.2 Failure mechanism discussion

Fig. 6(b) and Fig. 6(c) show the CB specimen before and after testing, respectively. It is clear that the specimen failed as expected at $P=60.73$ kN by a major shear crack with 45° inclination. The crack initiated under the loading point and propagated to the edge of the beam near the support.

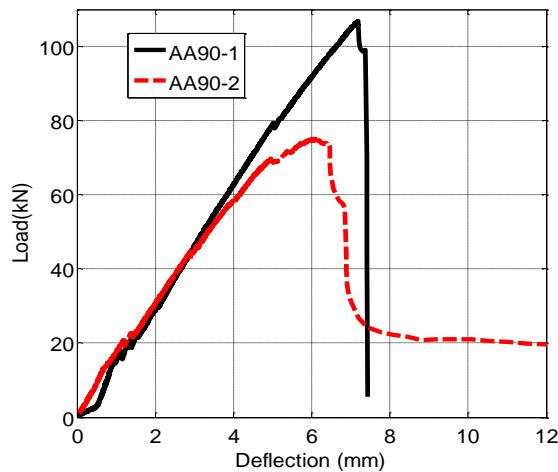
4.2 AA90 Beams

4.2.1 Strength and Load-deflection response

Specimens AA90 were tested under four-point bending as shown in Fig. 7(a). The ultimate load capacity of specimens AA90-1 and AA90-2 were 106.83 kN and 75.03 kN, respectively as presented in Table 6 and shown in Fig. 7 (b). Thus, there is an increase in the load carrying capacity of the strengthened AA90 beams over the CB specimen by 75.92% for AA90-1 and 23.5% for AA90-2. Fig. 7(b) shows the load-deflection response of AA90-1 and AA90-2 tested specimens. It was observed from the load-deflection curve that the deflection at ultimate load of specimen AA90-1 and AA90-2 were $\delta_u = 7.18$ mm and $\delta_u = 6.10$ mm, respectively.



(a) Vertical AA strips - AA90-1 and AA90-2



(b) Load-deflection for AA90-1 and AA90-2



AA90-1



AA90-2

(c) Failure mode – crack at 45°

Fig. 7. Specimens with vertical AA plates (AA90)

4.2.2 Failure mechanism discussion

Both specimens (AA90-1, AA90-2) failed by major shear cracks as shown in Fig. 7(c). In specimen AA90-1, the shear crack started at the point of the application of the load and propagated horizontally above some AA plates and changed to 45° inclination towards the support as shown in Fig. 7(c). The two AA plates near the loading point captured the shear cracks and forced the crack to take place as horizontal crack above the AA plates which resulted in higher load carrying capacity compared to AA90-2 specimen. AA90-2 failed by a major shear crack at 45° inclination as expected and it is formed from the point of application of the load to the edge of the beam near the support as shown in Fig.7(c).

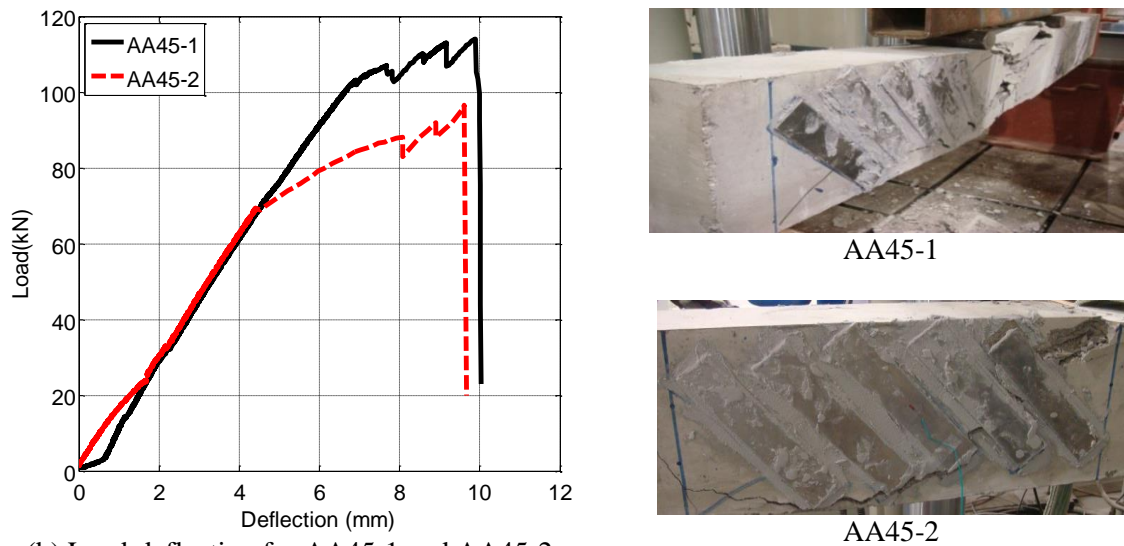
4.3 AA45 Beams

4.3.1 Strength and Load-deflection response

The ultimate load capacity of specimens AA45-1 and AA45-2 were 114.74 kN and 96.75 kN, respectively as shown in Table 6. Thus, there is an increase in the load carrying capacity of the strengthened AA45 beams over the CB by 88.9% for AA45-1 and 59.3% for AA45-2. Fig. 8(a) and 8(c) shows the strengthened specimens before and after testing. The load versus mid-span deflection response of AA45-1 and AA45-2 tested specimens are presented in Fig. 8(b). It was observed from the load-deflection curve of Fig. 8(b) that the deflection at ultimate load of specimen AA45-1 and AA45-2 were $\delta_u = 9.80$ mm and $\delta_u = 9.60$ mm, respectively.



(a) 45° AA Strips – AA45-1 and AA45-2



(b) Load-deflection for AA45-1 and AA45-2

(c) Failure mode – crack at 45°

Fig. 8. Specimens with AA plates at 45° (AA45)

4.3.2 Failure mechanism discussion

As presented in Fig. 8(c), specimen AA45-1 failure mechanism started with a minor shear crack that initiated at the loading point, and then got blocked by the adjacent AA plates and resulted in crushing of concrete at the compression zone near the loading point. This resulted in higher load carrying capacity compared to AA45-2 as indicated in the load-deflection curve shown in Fig. 8(b). Specimen AA45-2 failed by a major shear crack that zigzagged near the ends and around some of the AA plates and resulted in de-bonding of two AA plates near the point of application of the load as shown in Fig. 8(c).

4.4 AADP Beam

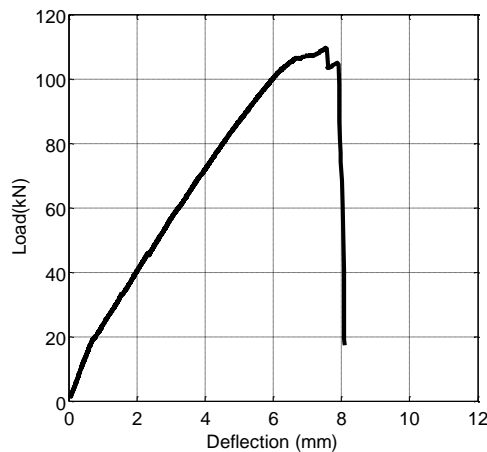
4.4.1 Strength and Load-deflection response

Fig. 9(a) shows the AADP specimen before testing. Specimen AADP was tested under four-point bending as well. The ultimate load capacity of specimen AADP was 109.55 kN as shown in Table 6. Thus, there is an increase in the load carrying capacity of the strengthened AADP

specimen over the CB specimen by 80.4%. Fig. 9(b) shows the load-deflection response of AADP specimen. It was observed from the load-deflection curve of Fig. 9(b) that the deflection at ultimate load of specimen AADP was $\delta_u = 7.53$ mm.



(a) Diagonal Plate bonded to the side -AADP



(b) Load-deflection for AADP



(c) Failure mode – crack at 20°

Fig. 9. Specimen with diagonal AA plate (AADP)

4.4.3 Failure mechanism discussion

This beam's behavior was different from the other strengthened specimens (AA90 and AA45). As shown in Fig 9 (c), the beam failed by a truss action in a combined shear and flexural mode due to the diagonally bonded plates that acted as tension ties. The beam failed by a major diagonal shear crack, inclined at an angle of about 20° as shown in Fig. 9(c), which is way smaller than the typical failure angle of 45°. The truss action created by the diagonal plates

(tension ties) enhanced the beam's performance and resulted in higher load than the calculated beam flexural capacity of 98 kN which is also higher than CB and AA90. Thus, such strengthening configuration of diagonally attached plates increased both the flexural and shear capacities of the RC beam specimen.

4.5 Summary of results

The load versus mid-span deflection curves of all tested specimens are plotted in Fig. 10. As presented earlier and summarized below, there is an increase in the load carrying capacity of AA strengthened beams ranging between 23.5% and 88.9%. This verifies that the use of AA plates as an external reinforcement for concrete beams is highly effective technique in increasing the beam shear capacity. It has also achieved a decrease in shear cracks during the loading process. The highest increase was reached by the AA-45 specimens which is a result of having the plates bonded perpendicular to the expected cracks' direction. In addition, AA-90 specimens and AADP beam achieved an average increase in the load carrying capacity of 49.7% and 80% respectively.

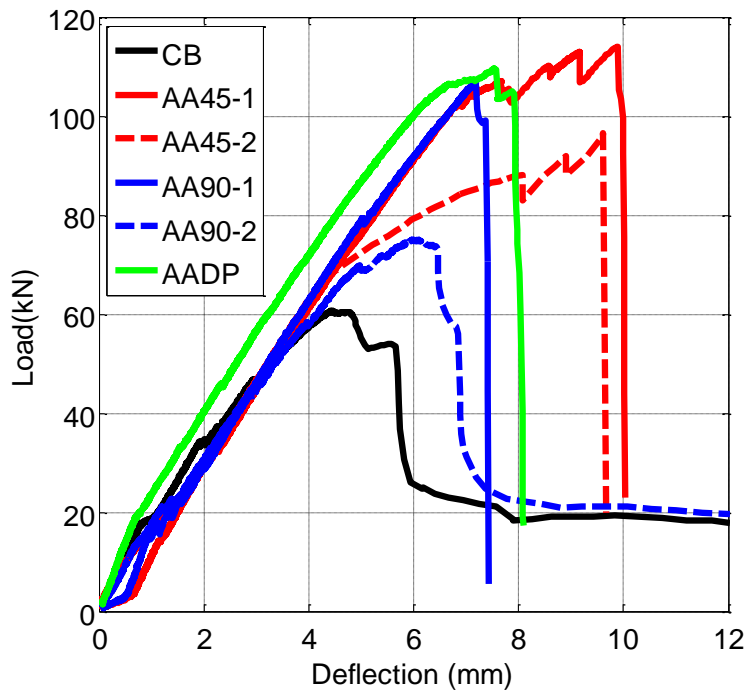


Fig. 10 Load vs deflection for all tested beams

It is worth mentioning that there is a considerable difference between the magnitude of the ultimate load of AA90-1 and AA90-2 and to some extent between that of AA45-1 and AA45-2. This difference is the result of: (1) the un-even surface roughness resulting from the un-even manual grinding of the AA plane surface; (2) the amount and thickness of the epoxy used to fill the un-even rough surfaces. The variation in AA surface roughness and the amount of epoxy used affected both the magnitude of the ultimate load and the failure mode of identical specimens. For consistent results, even grindings of the AA surface is needed and accordingly similar amount of epoxy can be maintained which will produce more consistent results. Such even surface roughness can be achieved by using a CNC machine for grinding or grooving.

5. Prediction of shear capacity using different FRP codes

Many analytical models have been developed to predict the shear capacity of RC beams strengthened with FRP sheets, FRP plates, and steel plates. Equations developed by ACI 440 [49], FIB14 [50], the concrete society in the UK (TR55) [51] and the Simplified Modified Compression Field Theory (SMCFT) [52] codes for FRP plates will be applied to predict the shear capacity of the beams strengthened with AA plates. These equations will be applied on the specimens with AA plates oriented at angles of 90° and 45° from the beam's longitudinal axis and sample calculations will be presented for each equation.

5.1 ACI 440 Predictions

ACI 440.2R-08 [49] is the American guide for the design and construction of externally bonded FRP systems for strengthening concrete structures. Fig. 11 shows some of the dimensions and variables that are used in predicting the FRP contribution to the shear capacity of strengthened RC beams. Equation (1), which is developed for FRP, has been used to predict the shear strength of the RC beams strengthened with AA plates. The effective thickness of the AA plate is assumed to be equal to 1.5 mm because of the small reduction due to grinding.

$$V_n = V_c + V_s + \Psi V_f \quad (1)$$

$$V_c = 0.17 \sqrt{f'_c} b_w d \quad (2)$$

$$V_f = \frac{A_{fv} f_{fe} (\sin \alpha + \cos \alpha) d_{fv}}{S_f} \quad (3)$$

$$A_{fv} = 2nt_f w_f = 2(1)(1.5)(50) = 150 \text{ mm}^2$$

$$k_1 = \left(\frac{f'_c}{27.6} \right)^{\frac{2}{3}} = \left(\frac{30}{27.6} \right)^{\frac{2}{3}} = 1.0515$$

$$L_e = \frac{23300}{(nt_f E_f)^{0.58}} = \frac{23300}{(1*1.5*70000)^{0.58}} = 28.51 \text{ mm}$$

$$k_2 = \frac{d_{fv} - 2L_e}{d_{fv}} = \frac{190 - 2(28.51)}{190} = 0.6998$$

$$k_v = \frac{k_1 k_2 L_e}{11900 \varepsilon_{fu}} = \frac{(1.0515)(0.6998)(28.51)}{11900*(146.3/70000)} = 0.8436 \leq 0.75 \rightarrow k_v = 0.75$$

$$\varepsilon_{fe} = k_v \varepsilon_{fu} = 0.75(146.3/70000) = 0.0015675 \leq 0.004$$

$$f_{fe} = \varepsilon_{fe} E_f = 0.0015675(70000) = 109.725 \text{ MPa}$$

$$V_f = \frac{A_{fv} f_{fe} (\sin \alpha + \cos \alpha) d_{fv}}{S_f} = \frac{150(109.725) * (\sin 1.5707 + \cos 1.5707)(190)}{(128)} = 24.43 \text{ kN}$$

$$V_c = 0.17 \sqrt{f'_c} b_w d = 0.17 \sqrt{29.76} * 150 * 200 = 27.82$$

$$V_n = V_c + V_s + \Psi V_f = 27.82 + 0 + (1)(24.43) = 52.25 \text{ kN}$$

$$P_n = 2 V_n = 2 * 52.25 = 104.5 \text{ kN}$$

where,

V_f nominal shear strength provided by FRP plates (N)

V_c nominal shear strength provided by concrete (N)

V_s nominal shear strength provided by shear reinforcement (N)

Ψ_f additional FRP strength-reduction factor

A_{fv} area of FRP shear reinforcement with spacing s , (mm^2)

f_{fe} effective stress in the FRP; stress level attained at section failure, (MPa)

d_{fv} effective depth of the FRP shear reinforcement, (mm)

ε_{fe} effective strain level in FRP reinforcement attained at failure, (mm/mm)

- L_e active bond length of FRP laminates, (mm)
- ε_{fu} ultimate rupture strain of FRP reinforcement, (mm/mm)
- E_f tensile modulus of elasticity of FRP plates, (MPa)
- n number of plies of FRP reinforcement
- b_w web width or diameter of circular section, (mm)
- w_f width of FRP reinforcing plies, (mm)
- t_f nominal thickness of one ply of FRP reinforcement, (mm)

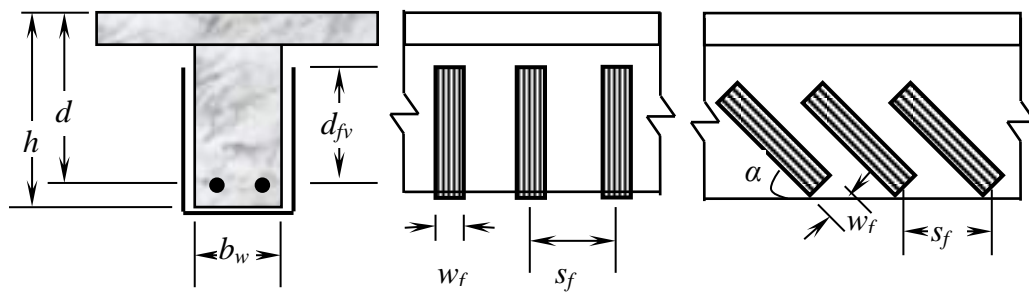


Fig. 11. Dimensional variables for externally bonded FRP [48]

5.2 International federation of structural concrete (FIB 14) Predictions

International federation of structural concrete (FIB 14) [50] explains the design and use of externally bonded fiber reinforced polymer reinforcement (FRP EBR) for reinforced concrete structures. According to FIB14, the following design guidelines are recommended to calculate the FRP contribution to the shear capacity of RC beams. The shear strength of reinforced concrete beams externally strengthened with FRP laminates is calculated using Eq. 4 according to the FIB14 design guidelines.

$$V_{Rd} = V_{cd} + V_{wd} + V_{fd} \quad (4)$$

$$V_{fd} = 0.9\varepsilon_{fd,e}E_{fu}\rho_f b_w d(\cot \theta + \cot \alpha) \sin \alpha \quad (5)$$

$$\rho_f = \left(\frac{2t_f}{b_w} \right) \left(\frac{b_f}{s_f} \right) = \left(\frac{2*1.5}{150} \right) \left(\frac{50}{128} \right) = 0.0078125$$

$$\varepsilon_{fe} = \min \left\{ \left[0.65 \left(\frac{(f_{cm})^{2/3}}{E_{fu}\rho_f} \right)^{0.56} \right] \times 10^{-3} \text{ or } 0.17 \left(\frac{(f_{cm})^{2/3}}{E_{fu}\rho_f} \right)^{0.3} \varepsilon_{fu} \right\}$$

Since no fracture occurred, the first part of the equation applied

$$= \left[0.65 \left(\frac{(37.2)^{2/3}}{70*0.0078125} \right)^{0.56} \right] \times 10^{-3} = 0.003516$$

Assuming $k = 0.8$ and $\gamma_f = 1.5$

$$\varepsilon_{fd,e} = 0.8 * 0.003516 / 1.5 = 0.001875$$

$$\cot \theta = \cot 45 = 1$$

$$\cot \alpha = \cot 90 = 0$$

$$\sin \alpha = \sin 90 = 1$$

$$\begin{aligned} V_{fd} &= 0.9\varepsilon_{fd,e}E_{fu}\rho_f b_w d(\cot \theta + \cot \alpha) \sin \alpha \\ &= 0.9(0.001875)(70000)(0.0078125)(150)(200)(1+0) * 1 = 27.685 \text{ kN} \end{aligned}$$

$$V_{Rd} = V_{cd} + V_{wd} + V_{fd} = 27.82 + 27.685 = 55.505 \text{ kN}$$

$$P_n = 2 * V_{Rd} = 2 * 55.505 = 111.01 \text{ kN}$$

where,

V_{fd} FRP contribution to shear capacity

V_{cd} concrete contribution to shear capacity

$\varepsilon_{fd,e}$ design value of the effective FRP strain

E_{fu} elastic modulus of FRP in the principle fiber orientation

ρ_f FRP reinforcement ratio equal to $\frac{2t_f \sin \alpha}{b_w}$ for continuously bonded shear reinforcement

or $\left(\frac{2t_f}{b_w}\right)\left(\frac{b_f}{s_f}\right)$ for FRP reinforcement in the form of strips

b_w minimum width of cross section over the effective depth

b_f width of the strips of the bonded reinforcement (mm)

s_f spacing between the strips of the bodned reiforcment (mm)

t_f thickness of bonded reinforcement (mm)

d effective depth of cross section (mm)

θ angle of diagonal crack with respect to the member axis, assumed equal to 45°

α angle between principal fibre orientation and longitudinal axis of member

k reduction factor (k=0.8)

$\gamma_w = \gamma_{fb}$ partial safety factor (if failure involves fracture)

5.3 The concrete society in the UK (TR55)

TR55 [51] is the design guidance for strengthening concrete structures using fiber composite materials in UK. Equation 6 is used to predict the shear strength of RC beams externally strengthened with FRP sheets and plates according to the TR55 design guidelines. Details of the elements of this equation are given in TR55.

$$V_{Re} = V_{Rc} + V_{RI} + V_{Rf} \quad (6)$$

$$V_{Rf} = \left(\frac{1}{\gamma_{mF}}\right) A_{fs} (E_{fd} \varepsilon_{fe}) \sin \beta (1 + \cot \beta) \left(\frac{d_f}{S_f}\right)$$

$$\rho_f = \left(\frac{2t_f}{b_w} \right) \left(\frac{b_f}{s_f} \right) = \left(\frac{2*1.5}{150} \right) \left(\frac{50}{128} \right) = 0.0078125$$

$$L_e = \frac{461.3}{(t_f E_{fd})^{0.58}} = \frac{461.3}{(1.5 * 70)^{0.58}} = 31.024$$

$$w_{fe} = d_f - 2L_e = 200 - 2*31.024 = 137.95$$

$$A_{fs} = 2t_f w_{fe} = 2*1.5*137.95 = 413.858$$

Assuming $\gamma_{mf} = 1$

$$\varepsilon_{fu} = \frac{\varepsilon_{fk}}{\gamma_{mf}} = \frac{(146.3/70000)}{1} = 0.00209$$

$$\begin{aligned} \varepsilon_{fe} &= \varepsilon_{fu} \left[0.5622(\rho_f E_{fd})^2 - 1.2188\rho_f E_{fd} + 0.778 \right] \\ &= (146.3/70000) * \left[0.5622(0.0078125 * 71)^2 - 1.2188 * 0.0078125 * 70 + 0.778 \right] = 0.000584 \end{aligned}$$

$$\varepsilon_{fe} = \frac{0.0042 \left[0.835(f_{cu})^{2/3} \right] \times w_{fe}}{(E_{fd} t_f)^{0.58} \times d_f} = \frac{0.0042 \left[0.835(37.2)^{2/3} \right] \times 137.95}{(70 * 1.5)^{0.58} \times 200} = 0.001813$$

$$\begin{aligned} V_{Rf} &= \left(\frac{1}{\gamma_{mF}} \right) A_{fs} (E_{fd} \varepsilon_{fe}) \sin \beta (1 + \cot \beta) \left(\frac{d_f}{S_f} \right) \\ &= \left(\frac{1}{1} \right) (413.858)(70 * 0.000584) \sin 90 (1 + \cot 90) \left(\frac{200}{128} \right) = 26.45 \text{ kN} \end{aligned}$$

$$V_{Re} = V_{Rc} + V_{Rl} + V_{Rf} = 27.82 + 26.45 = 54.27 \text{ kN}$$

$$P_n = 2 * V_{Rd} = 2 * 54.27 = 108.55 \text{ kN}$$

Where,

V_{Rf} FRP contribution to shear capacity

V_{Rc} concrete contribution to shear capacity

A_{fs} area of FRP shear reinforcement

E_{fd} design Elastic modulus of FRP (GPa)

- ε_{fu} design ultimate failure strain in FRP
- w_{fe} effective width of the FRP
- s_f spacing between the strips of the bonded reinforcement (mm)
- ρ_f FRP reinforcement ratio equal to $\frac{2t_f \sin \alpha}{b_w}$ for continuously bonded shear reinforcement
- or $\left(\frac{2t_f}{b_w}\right)\left(\frac{b_f}{s_f}\right)$ for FRP reinforcement in the form of strips
- b_w minimum width of cross section over the effective depth
- w_f width of the strips of the bonded reinforcement (mm)
- s_f spacing between the strips of the bonded reinforcement (mm)
- t_f thickness of bonded reinforcement (mm)
- d effective depth of cross section (mm)
- f_{cu} cube strength of concrete (MPa)
- β angle between principal fibre orientation and longitudinal axis of member
- γ_{mF} partial safety factor for FRP

5.4 Simplified Modified Compression Field Theory Predictions:

The Simplified Modified Compression Field Theory (SMCFT), originally developed by Bentz et al. [52] and adopted by AASHTO LRFD 2014, is used here as presented in Eq. 7 to predict the shear capacity of the reinforced concrete beams strengthened in shear with AA plates.

An iterative procedure is required to perform the calculations of the SMCFT. The initial estimates of V_c and V_{AA} are determined from the ACI 318-14 equations of V_c and V_s respectively. Once the shear capacity of the section is calculated (V_n), the strain in the steel (ε_s) is

computed. Once determined, (ε_s) is used to compute β and θ . These two quantities are then used to update the V_c and V_{AA} then V_n . The process is then repeated until the solution converges to the correct V_n . The debonding strain of an FRP sheet or plate is estimated based on the ACI440.2R-08 suggested values of the lesser of 0.004 and $0.75\varepsilon_{fu}$. Since the AA plate does not show signs of yielding upon shear failure, the rupture strain ε_{fu} of FRP is replaced with the yielding strain of the AA plate ε_{yAA} . Accordingly, the debonding strain of the AA plate is estimated to $0.75\varepsilon_{yAA} = 0.75 \times 0.0021 = 0.001575$. Furthermore, the effective thickness of the AA plate is assumed to be equal to 1.5 mm because of the small reduction due to grinding. Below, the SMCFT equations are given along with the calculations to predict the capacity of the AA90 specimen in order to demonstrate the analytical prediction procedure. Calculations will be given for the last iteration at convergence in case the shear crack forms at the most critical section under the point load at the section of maximum moment.

$$V_n = V_C + V_S + V_{AA} \quad (7)$$

$$V_{AA} = \frac{A_v f_{eAA} d_v (\cot \theta + \cot \alpha) \sin \alpha}{S} \quad (8)$$

$$V_C = \beta \sqrt{f_c'} b_v d_v \quad (9)$$

$$\varepsilon_s = \frac{\frac{|M|}{d_v} + 0.5N + V_n}{A_s E_s} = 0.002653$$

$$\beta = \frac{0.4}{1 + 750 \varepsilon_s} \frac{1300}{1000 + s_{xe}} = 0.1509$$

$$\theta = (29^\circ + 3500 \varepsilon_s) = 38.28^\circ$$

$$s_{xe} = s_x \frac{35}{a_g + 16} = 153 \text{ mm}$$

$$d_v = \text{Maximum} \left(\begin{array}{l} 0.72h = 180 \text{ mm} \\ 0.9d = 180 \text{ mm} \\ M_n / A_y f_y = 168.7 \text{ mm} \end{array} \right) = 180 \text{ mm}$$

$$V_C = \beta \sqrt{f'_c} b_v d_v = 22.22 \text{ kN}$$

$$V_S = \frac{A_v f_y d_v (\cot \theta + \cot \alpha) \sin \alpha}{S} = 0$$

$$V_{AA} = \frac{A_v f_{eAA} d_v (\cot \theta + \cot \alpha) \sin \alpha}{S} = 29.46 \text{ kN}$$

$$V_n = V_C + V_S + V_{AA} = 22.22 + 0 + 29.46 = 51.68 \text{ kN}$$

$$P_n = 2 V_n = 103.37 \text{ kN}$$

Where

d_v = effective shear depth taken as the distance, measured perpendicular to the neutral axis, between the tensile resultant and compressive force due to flexure. It needs not be taken to be less than the greater of 0.9d or 0.72h.

β = factor indicating ability of diagonally cracked concrete to transmit tension and shear

θ = angle of inclination of diagonal compressive stresses or shear crack (°)

α = angle of inclination of transverse reinforcement to longitudinal axis (°).

S_x = the lesser of d_v or the vertical distance between horizontal layers of longitudinal crack control reinforcement.

a_g = maximum aggregate size and it has to equal zero when $f'_c \geq 69 \text{ MPa}$

M = moment in N.mm

V = shear force in Newton

N = axial force, taken as positive if tensile and negative if compressive in Newton

A_s = area of non-prestressed steel on the flexural tension side of the section. This is considered to be the area of flexural reinforcement under the original geometric centroid of the section.

E_s = modulus of elasticity of steel in ksi (MPa).

According to this theory, the control beam is predicted to have $V_n = V_c = 31.93$ kN when the shear crack is initiated at the loading point near mid-span. This corresponds to $P_n = 63.86$ kN which is comparable to the 60.73 kN ultimate load.

For the beam AA-90, it is predicted to have $V_n = V_c + V_{AA} = 51.68$ kN when the shear crack starts at the loading point near mid-span. This corresponds to $P_n = 103.37$ kN which is slightly lower than the 106.94 kN ultimate load of Beam AA-90-1. On the other hand, Beam AA90-2 failed prematurely at 75 kN which may be attributed to thinner AA plate thickness due to the manual grinding.

For the Beam AA-45, it is predicted to have $V_n = V_c + V_{AA} = 57.27$ kN when the shear crack starts at the loading point near mid-span. This corresponds to $P_n = 114.55$ kN which is matching the ultimate load of Beam AA-45-1 that failed at 114.74 kN. On the other hand, the failure load of Beam AA-45-2 is found to be 96.75 kN. This reduction in ultimate load may also be attributed to thinner AA plate thickness due to the manual grinding. In general the SMCFT is found to be accurate enough in predicting the ultimate shear capacity of the strengthened beams.

5.5 Summary of the results

The four shear strength prediction code equations were used to predict the shear capacity of concrete sections and hence compute the ultimate shear strength of the tested specimens. Table 7 and Fig. 12 show the results of the statistical measurements of the predictions of the ACI, TR55, FIB14 and SMCFT codes. The ultimate predicted load (P_{pre}) is equal to twice the shear capacity of the reinforced concrete beam predicted by one of the codes such as V_n in ACI440 and

SMCFT, V_{Rd} in FIB14 or V_{Re} in TR55. The recommended additional reduction factor (Ψ_f) in the ACI equation was assumed to be 1.0 since the values suggested in the code are based on a reliability analysis of FRP data. Similarly in TR55 predictions, the partial safety factor ($\gamma_f = \gamma_{fb}$) was not applied since the values suggest are based on the FRP laminates mechanical of properties and method of manufacture. For the FIB14 predictions, a material safety factor of 1.5 was applied for the concrete since the bond failure occurred in the concrete. Further investigation is required for the safety factors applied in each code for the AA plates contribution is the shear capacity of the RC beams.

As observed, the Mean Absolute Percent Error (MAPE) of the prediction by each of the four codes is relatively comparable with maximum MAPE of 48.78% depicted by FIB14 prediction for specimen AA90-2. The average of MAPE for all code predictions ranges between 14.94% and 27.45% which indicates that they have comparable accuracy, with the SMCFT appears to be the most accurate and the FIB14 is the least accurate in predicting the shear strength of the tested beams.

Table 7 Measured and predicted ultimate loads of AA90 and AA45 Specimens

Specimen	Measured (Exp.) (kN)	ACI 440 [49]			FIB 14 [50]			TR55 [51]			SMCFT [52]		
		Pred. ($\Psi_f=1$) (kN)	$P_{exp}/$ P_{pre}	MAPE (%)	Pred. (No k) (kN)	$P_{exp}/$ P_{pre}	MAPE (%)	Pred (3.5) (kN)	$P_{exp}/$ P_{pre}	MAPE (%)	Pred. (kN)	$P_{exp}/$ P_{pre}	MAPE (%)
AA90-1	106.83	104.51	1.02	1.75	111.02	0.96	4.49	108.55	0.99	1.40	103.37	1.03	3.24
AA90-2	75.03	104.51	0.71	39.90	111.02	0.67	48.78	108.55	0.69	44.38	103.37	0.73	37.77
AA45-1	114.74	124.74	0.92	9.20	133.96	0.85	17.35	130.46	0.88	13.35	114.55	1.00	0.17
AA45-2	96.75	124.74	0.77	29.51	133.96	0.72	39.17	130.46	0.74	34.43	114.55	0.84	18.59
Average			0.86	20.09		0.80	27.45		0.83	23.39		0.9	14.94

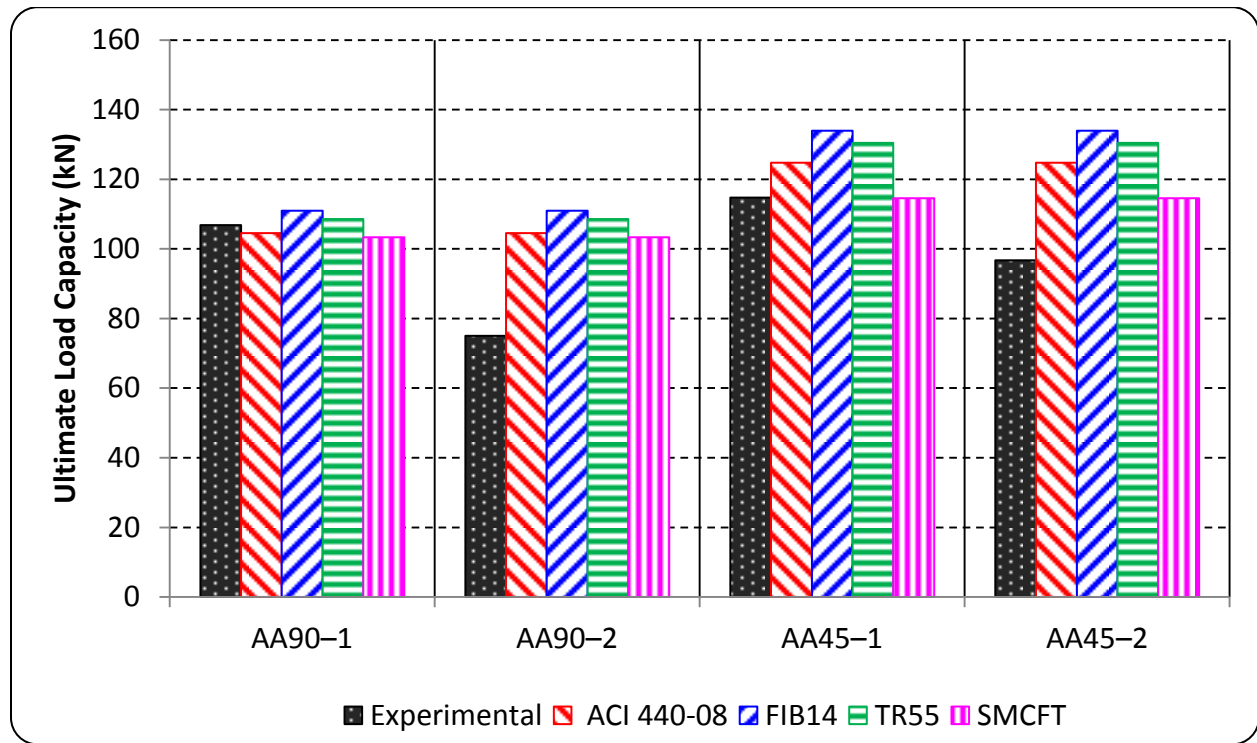


Fig. 12 Measured and predicted ultimate loads

6. Conclusions

This paper presents the result of five RC beams strengthened in shear with externally bonded AA plates with different orientations and spacing. Based on this investigation the following observations and conclusions can be made:

1. Aluminum alloy plates can be used to externally strengthen reinforced concrete beams in shear. Based on the result of this investigation, the increase in shear capacity ranged between 24% and 89%. Therefore, using Aluminum plates is a highly effective technique in increasing the beam shear capacity.
2. Orientation of AA plates, as external strengthening material, has a major effect on the load-carrying capacity of the strengthened RC beams. As observed, the 45° AA plate

orientation is more effective than the 90° plate orientation in increasing the beam's shear capacity. However, this conclusion is valid for gravity loads or loads applied vertically downward as is the case in this test setting.

3. Codes developed for FRP (ACI440, FIB14 and TR55, SMCFT) can be used to predict, to some degree of accuracy, the shear capacity of beams strengthened with externally bonded AA plates, however, more specialized equations need to be developed for AA. This requires further experimental studies.
4. The result of this investigation validates the viability of using AA plates as alternative to the prevailing FRP laminates and steel plate as externally bonded shear strengthening material.
5. Further experimental studies will be required to confirm the effectiveness of using bonded AA plates in shear strengthening and also to investigate the effect of different orientations, grades, and thicknesses of AA plates in shear strengthening of RC beams.

Acknowledgement

The support for the experimental part of the research presented in this paper had been provided by the American University of Sharjah. The support is gratefully acknowledged. The views and conclusions, expressed or implied, in this paper are those of the authors and should not be interpreted as those of the sponsor. We want to acknowledge Engineer Arshi Faridi and Ansari for their help in conducting the experimental program.

References

- [1] Adhikary, B. B., Mutsuyoshi, H., & Sano, M. (2000). Shear strengthening of reinforced concrete beams using steel plates bonded on beam web: experiments and analysis. *Construction and Building Materials*, 14(5), 237-244.
- [2] Al-Sulaimani, G. J., Sharif, A., Basunbul, I. A., Baluch, M. H., & Ghaleb, B. N. (1994). Shear repair for reinforced concrete by fiberglass plate bonding. *Structural Journal*, 91(4), 458-464.
- [3] Chajes, M. J., Januszka, T. F., Mertz, D. R., Thomson Jr, T. A., & Finch Jr, W. W. (1995). Shear strengthening of reinforced concrete beams using externally applied composite fabrics. *ACI Structural Journal*, 92(3).
- [4] Triantafillou, T. C. (1998). Shear strengthening of reinforced concrete beams using epoxy-bonded FRP composites. *ACI Structural Journal*, 95(2).
- [5] Täljsten, B., & Elfgrén, L. (2000). Strengthening concrete beams for shear using CFRP-materials: evaluation of different application methods. *Composites Part B: Engineering*, 31(2), 87-96.
- [6] Khalifa, A., & Nanni, A. (2000). Improving shear capacity of existing RC T-section beams using CFRP composites. *Cement and Concrete Composites*, 22(3), 165-174.
- [7] Bakis, C., Bank, L. C., Brown, V., Cosenza, E., Davalos, J. F., Lesko, J. J., & Triantafillou, T. C. (2002). Fiber-reinforced polymer composites for construction-state-of-the-art review. *Journal of Composites for Construction*, 6(2), 73-87.
- [8] Täljsten, B. (2003). Strengthening concrete beams for shear with CFRP sheets. *Construction and Building Materials*, 17(1), 15-26.

- [9] Bousselham, A., & Chaallal, O. (2004). Shear strengthening reinforced concrete beams with fiber-reinforced polymer: Assessment of influencing parameters and required research. *ACI Structural Journal*, 101(2).
- [10] Zhang, Z., & Hsu, C. T. T. (2005). Shear strengthening of reinforced concrete beams using carbon-fiber-reinforced polymer laminates. *Journal of Composites for Construction*, 9(2), 158-169.
- [11] Monti, G. (2007). Tests and design equations for FRP-strengthening in shear. *Construction and Building Materials*, 21(4), 799-809.
- [12] Sundararaja, M. C., & Rajamohan, S. (2009). Strengthening of RC beams in shear using GFRP inclined strips—An experimental study. *Construction and building materials*, 23(2), 856-864.
- [13] Belarbi, A., Bae, S. W., & Brancaccio, A. (2012). Behavior of full-scale RC T-beams strengthened in shear with externally bonded FRP sheets. *Construction and Building Materials*, 32, 27-40.
- [14] Colalillo, M. A., & Sheikh, S. A. (2012). Seismic retrofit of shear-critical reinforced concrete beams using CFRP. *Construction and Building Materials*, 32, 99-109.
- [15] Dong, J. F., Wang, Q. Y., & Guan, Z. W. (2012). Structural behaviour of RC beams externally strengthened with FRP sheets under fatigue and monotonic loading. *Engineering Structures*, 41, 24-33.
- [16] Baggio, D., Soudki, K., & Noël, M. (2014). Strengthening of shear critical RC beams with various FRP systems. *Construction and Building Materials*, 66, 634-644.

- [17] Mofidi, A., & Chaallal, O. (2014). Tests and design provisions for reinforced-concrete beams strengthened in shear using FRP sheets and strips. *International Journal of Concrete Structures and Materials*, 8(2), 117-128.
- [18] Baghi, H., Barros, J. A., Rezazadeh, M., & Laranjeira, J. (2015). Shear Strengthening of Damaged RC Beams with Hybrid Composite Plates. *Journal of Composites for Construction*, 04015041.
- [19] Panigrahi, A. K., Biswal, K. C., & Barik, M. R. (2014). Strengthening of shear deficient RC T-beams with externally bonded GFRP sheets. *Construction and Building Materials*, 57, 81-91.
- [20] Li, A., Assih, J., & Delmas, Y. (2001). Shear strengthening of RC beams with externally bonded CFRP sheets. *Journal of Structural Engineering*, 127(4), 374-380.
- [21] Aykac, S., Kalkan, I., Aykac, B., Karahan, S., & Kayar, S. (2012). Strengthening and repair of reinforced concrete beams using external steel plates. *Journal of Structural Engineering*, 139(6), 929-939.
- [22] Barnes, R. A., Baglin, P. S., Mays, G. C., & Subedi, N. K. (2001). External steel plate systems for the shear strengthening of reinforced concrete beams. *Engineering structures*, 23(9), 1162-1176.
- [23] Adhikary, B. B., & Mutsuyoshi, H. (2006). Shear strengthening of RC beams with web-bonded continuous steel plates. *Construction and Building Materials*, 20(5), 296-307.
- [24] Adhikary, B. B., & Mutsuyoshi, H. (2006). Shear strengthening of reinforced concrete beams using various techniques. *Construction and Building Materials*, 20(6), 366-373.

- [25] Barnes, R. A., & Mays, G. C. (2006). Strengthening of reinforced concrete beams in shear by the use of externally bonded steel plates: Part 1–Experimental program. *Construction and Building Materials*, 20(6), 396-402.
- [26] Abdalla, J.A., Abu-Obeidah, A. and Hawileh, R.A. (2011). Behavior of Shear Deficient Reinforced Concrete Beams with Externally Bonded Aluminum Alloy Plates. The 2011 World Congress on Advances in Structural Engineering and Mechanics (ASEM\11+ Congress, Seoul, South Korea, September 18- 23.
- [27] Abu-Obeidah, A., Hawileh, R. A., and Abdalla, J. A. (2012), "Finite Element Modeling of Shear Deficient Beams Bonded with Aluminum Plates." Proceedings of the 11th International Conference on Computational Structures Technology, Civil-Comp Press, Stirlingshire, Scotland, paper 1, 2012, Dubrovnik, Croatia, September 4-9.
- [28] Abu-Obeidah, A., Hawileh, R. A. and Abdalla, J. A. (2015). Finite element analysis of strengthened RC beams in shear with aluminum plates. *Computers & Structures*, 147, 36-46.
- [29] Chaallal, O., Nollet, M. J., & Perraton, D. (1998). Shear strengthening of RC beams by externally bonded side CFRP strips. *Journal of Composites for Construction*, 2(2), 111-113.
- [30] Grace, N. F., Sayed, G. A., Soliman, A. K., & Saleh, K. R. (1999). Strengthening reinforced concrete beams using fiber reinforced polymer (FRP) laminates. *ACI Structural Journal*, 96(5), 865-875.
- [31] Sim, J., Kim, G., Park, C., & Ju, M. (2005). Shear strengthening effects with varying types of FRP materials and strengthening methods. *ACI Special Publication*, 230.
- [32] Hawileh, R.A., Nawaz, W., Abdalla, J.A. and Saqan, E.I. (2015). Effect of Flexural CFRP Sheets on Shear Resistance of Reinforced Concrete Beams. *Composite Structures*, Vol. 122, pp. 468-476.

- [33] Hawileh, R., Nawaz, W., Abdalla, J., and Saqan, E. (2015). External Strengthening of Shear Deficient Reinforced Concrete Beams with Flexural CFRP Laminates." Response of Structures under Extreme Loading, Proceedings of the 5th International Workshop on Performance, Protection & Strengthening of Structures under Extreme Loading (PROTECT 2015), pp. 368-373, East Lansing, Michigan, June 28-30.
- [34] Nawaz, W., Hawileh, R.A., Saqan, E.I. and Abdalla, J.A. (2016). Effect of Longitudinal CFRP Plates on the Shear Strength of RC Beams. *ACI Structural Journal*, 113(3), 577-586.
- [35] Sato, Y., Ueda, T., Kakuta, Y., & Tanaka, T. (1996). Shear reinforcing effect of carbon fiber sheet attached to side of reinforced concrete beams. In *Proceedings of the 2nd International Conference on Advanced Composite Materials in Bridges and Structures, ACMBS-II, Montreal 1996*.
- [36] Umezu, K., Fujita, M., Nakai, H., & Tamaki, K. (1997). Shear behavior of RC beams with aramid fiber sheet non-metallic (FRP) reinforcement for concrete structures. Proceedings of the 3rd International Symposium on Non-Metallic (FRP) Reinforcement for Concrete Structures, October 14-16, 1997, Tokyo, Japan, pp: 491-498.
- [37] Mofidi, A., Chaallal, O., Benmokrane, B., & Neale, K. (2011). Performance of end-anchorage systems for RC beams strengthened in shear with epoxy-bonded FRP. *Journal of Composites for Construction*, 16(3), 322-331.
- [38] Altin, S., Anil, Ö., & Kara, M. E. (2005). Improving shear capacity of existing RC beams using external bonding of steel plates. *Engineering structures*, 27(5), 781-791.
- [39] Kissell, J. R., & Ferry, R. L. (1995). *Aluminum structures: a guide to their specifications and design*. 1st ed. New York, United States. John Wiley & Sons.

- [40] Dursun, T. and Soutis, C. (2014). Recent developments in advanced aircraft aluminium alloys. *Materials & Design*, 56, 862-871.
- [41] Mazzolani, F. and Feder M. (1995). *Aluminium Alloy Structures, Second Edition*: Publisher E & FN Spon.
- [42] Mazzolani, F. (2006). Structural Applications of Aluminium in Civil Engineering. *Structural Engineering International* 16(4), 280-285.
- [43] Soetens, F. (2010). Aluminium Structures in Building and Civil Engineering Applications, *Structural Engineering International* 20(4), 430-435.
- [44] Aluminum and Aluminum Alloys. Edited by Joseph R. Davis. ASM Speciality Handbook, 1993.
- [45] Aalco. (n.d.). Retrieved January 15, 2011, from <http://www.aalco.co.uk/datasheets>
- [46] Abdalla, J., Hraibb, F., Hawileha R., and Mirghania A. (2016). Experimental investigation of bond-slip behavior of aluminum plates adhesively bonded to concrete. *Journal of Adhesion Science and Technology*, DOI:10.1080/01694243.2016.1204741
- [47] ASTM Standard B928/B928M, (2002). Standard Specification for High Magnesium Aluminum-Alloy Products for Marine Service and Similar Environments. ASTM International, West Conshohocken, PA, 2002, www.astm.org.
- [48] Sika Construction Chemicals, Sikadur-30 LP, (2009). Adhesive for Bonding Reinforcement. Product Data Sheet, Sika Limited (Vietnam).
- [49] ACI, ACI 440.2-08: Guide for the Design and Construction of Externally Bonded FRP Systems for Strengthening Concrete Structures," Farmington Hills, MI, 2008.

- [50] FIB14 (2001). Externally bonded FRP reinforcement for RC structures. The international federation for structural concrete (CEB-FIB), technical report bulletin 14, Sika Services AG, Switzerland, 2001.
- [51] TR55 (2000). Design guidance for strengthening concrete structures using fibre composite materials. Concrete Society.
- [52] Bentz EC, Vecchio FJ, and Collins MP (2006). Simplified Modified Compression Field Theory for Calculating Shear Strength of Reinforced Concrete Elements. *ACI Structural Journal* 103(4), 614-624.

© 2016. This manuscript version is made available under the CC-BY-NC-ND 4.0 license <http://creativecommons.org/licenses/by-nc-nd/4.0/>